Materials Chemistry and Physics 223 (2019) 88–97

Contents lists available at ScienceDirect

Materials Chemistry and Physics

journal homepage: www.elsevier.com/locate/matchemphys

Degradation mechanism and way of surface protection of nickel nanostructures

E.Yu Kaniukov[a], A.E. Shumskaya[a], M.D. Kutuzau[a,*], V.D. Bundyukova[a], D.V. Yakimchuk[a], D.B. Borgekov[c,d], M.A. Ibragimova[c], I.V. Korolkov[d], ShG. Giniyatova[c], A.L. Kozlovskiy[c,d], M.V. Zdorovets[b,c,d]

[a] Scientific and Practical Materials Research Centre of the National Academy of Sciences of Belarus, Minsk, 220072, Belarus
[b] Ural Federal University Named After the First President of Russia B.N.Yeltsin, Ekaterinburg, Russian Federation
[c] L.N. Gumilyov Eurasian National University, Astana, Kazakhstan
[d] Laboratory of Solid State Physics, Institute of Nuclear Physics Astana, Kazakhstan

HIGHLIGHTS

- The influence of media with different pH (1...7) on nanotubes was studied.
- Nanotubes morphology and structure after interaction were analyzed.
- Ni nanotubes degradation mechanism was described.
- Degradation scheme: passivation → formation of point defects → pitting → destruction.
- Ways of surface protection with gold, organosilicon and polymer coatings were shown.

ARTICLE INFO

Keywords:
Nanostructures
Template synthesis
Nickel nanotubes
Degradation
Coatings
Surface protection
Functionalization

ABSTRACT

Stability of nanomaterials during their life cycle is a crucial problem of modern nanoscience. In order to understand the processes, which are going in the nanostructures, the comprehensive study of the influence of media with different acidity on the nickel nanotubes morphology and structure was carried out. On the base of the analysis of nanotubes characteristics, sequential evolution of degradation stages involving the surface passivation, formation of point defects, pitting and destruction of nanotubes walls was determined. The results are of importance for the wide range of potential nickel nanostructures applications, which are associated with their using in real-life conditions. To improve Ni nanostructures stability, the possible ways of surface protections from the aggressive environment effect and the routes of nanostructures covering with gold, organosilicon compounds and polymer coatings were considered. Demonstrated approaches for nanostructures covering provide an opportunity of surface functionalization for attaching of different molecules. It is useful for targeted delivery of drugs and genes, biodetection, bioseparation and catalysis application.

1. Introduction

Recently interest in the manufacture of nanowires (NWs) and nanotubes (NTs) increase due to their unique mechanical, optical, magnetic and electronic properties. NWs and NTs have a huge potential for application in nanoelectronic devices [1], for catalysis [2], high-density magnetic recording [3], bio-application [4,5]. To date a wide variety of methods for the tailored nanostructures (NSs) formation exists, such as electrochemical deposition [3,6], electron-beam lithography [7], chemical vapor deposition [8], pulsed laser deposition [9], and other methods [10–19]. Among the all range of synthesis methods, electrochemical deposition stands out, because it allows to control the structure, elemental and phase composition of the NSs by variation only of the deposition conditions [3,20,21].

For creation of NSs with a high aspect ratio, nickel is actively used today due to attractive physical and chemical properties. NSs based on Ni are promising for the design of optoelectronic elements, magnetic sensors, contrast liquids, drug delivery systems, storage of hydrogen and for direct use as chemical catalysts [22–26]. It should be noted that the presence of a hollow channel inside NTs gives some advantages over

* Corresponding author.
E-mail address: algerd1514@tut.by (M.D. Kutuzau).

https://doi.org/10.1016/j.matchemphys.2018.09.010
Received 15 February 2018; Received in revised form 15 June 2018; Accepted 1 September 2018
Available online 03 September 2018
0254-0584/

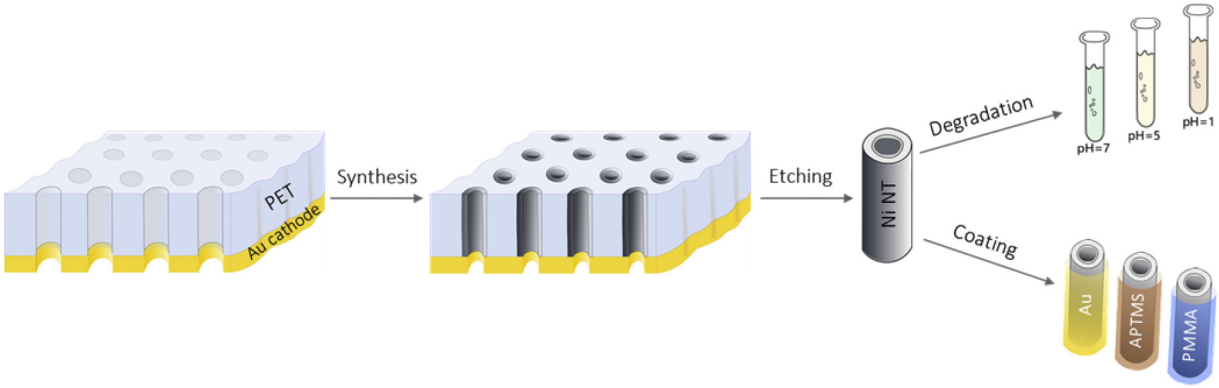

Fig. 1. Schematic representation of main stages of the work.

NWs: the specific surface area significantly increases, that is critical for catalysis applications. The absence of a magnetic core makes it possible to create NSs with a uniform magnetic field distribution [23], that is important for construction of microelectronic devices and memory elements. Due to the lower specific density NTs can float in liquids (including biological ones), that is important for bio-application, for example, for drugs delivery systems [24].

Mostly, oxidation is considerate as a negative process, which leads to degradation of the material and loss of their initial properties [29–31]. For example, the formation of nickel oxide and hydroxide in the volume of the NSs entails a change in the magnetic and electrical properties, it is critical for micro- and nanoelectronic applications. Degradation of nickel NSs in acidic and slightly acidic media with the formation of toxic nickel oxides can lead to cell apoptosis in case of bio-application [27]. Therefore, for most areas of use of nickel NSs, oxidation leading to the formation of dangerous compounds on the surface and in volume, as well as the destruction of NSs is undesirable. Nevertheless, the information about the changes occurring in nickel NSs during exposition in media with different acidity is fragmentary, and for NTs is practically absent, the study of the behavior of Ni NTs under the influence of media with different acidity is important task.

To prevent the oxidation and destruction of NSs various types of coatings are used. Generally, coatings impart chemical stability, mechanical strength and allow prolonging the service life of NSs. Moreover, it is possible to form new functional bonds for attaching tailored cargo. New properties of the nanomaterial will be determined by the uniformity of the coating and its reliability. There are three main ways of functionalizing the surface: inorganic (noble metals), organic (biocompatible polymers, organosilicon compounds) and composite ones.

Usually, for creation of a gold shell around metal NSs, two main methods are considered: (1) direct deposition of gold on the surface and (2) indirect deposition, through the “mediator” layer. Direct deposition of gold can be carried out from an aqueous solution or from an organic phase. The most common method is the deposition of gold atoms from chloride by the addition of sodium citrate [28]. The mediated method consists in step-by-step creation of a “mediator” layer on the magnetic nanostructure surface at the first stage, and after – in deposition of gold on its surface [29]. The advantage of this method is the ability to create a coating of a predefined thickness. It is achieved by simply repeating of described procedure.

Creation of organosilicon coatings on the surface of metallic NSs by silanization is an attractive way for surface protection. In this case silanol group of the silane coupling agents reacts with the surface [30] [31], by hydrolysis and polycondensation of $R{-}Si(C_xH_y)_3$ on the surface hydroxyl groups of metallic NSs. Organosilicon layer can be considered as an independent functionalizing layer or as a basis for creating other organic coatings. For further interaction with the target molecules, providing stable covalent bonds and forming a single-molecule thin layer on the metal surface, (3-Aminopropyl)triethoxysilane and (3-aminopropyl)trimethoxysilane are the most commonly used for this purpose. It is important to note that silane coupling agents can also be used to prevent aggregation of NSs.

For the surfaces functionalization with polymers there are a lot of methods in use. A radical polymerization method is possible, it could be carried out through a step of coating with an organosilicon compound and addition of a thermal initiator described in Ref. [32]. Thanks to this method, almost any polymer can be grafted. It is also possible to coat a polymer by mean of controlled radical polymerization of NSs surface in accordance with the atom transfer radical polymerization mechanism [33] or a direct reaction between hydroxide groups formed on the surface of NSs due to corrosion in weakly alkaline solutions and C = O bonds that are present in polymers through hydrogen bonds or covalent attachment of polymers with terminal SH-bonds [34]. The perspective method of creating protective layers is covering by hydrogel matrices [35], which allows to produce co-shell magnetic NSs with high biocompatibility, low friction, fast response, and spatial temporal control manipulation, as well as non-invasive and remote actuation [36].

In this work we study influence of media with different acidity on the nickel nanotubes morphology, composition and basic parameters of the crystal structure to understand the degradation mechanism and to show the possible ways of nanostructures surface protections from the environment effect with using of gold, (3-aminopropyl)trimethoxysilane and poly(methyl methacrylate) coatings.

1.1. Experimental part

Template synthesis of Ni NTs, study of the evolution of the morphology, composition and basic parameters of the crystal structure of NSs and their covering with various coatings, were carried out. The main scheme of investigations is shown on Fig. 1.

1.2. Nanotubes formation

Track-etched membranes with a thickness of 12 μm (pore diameter of 400 nm and density of 4×10^7 cm^{-2}) based on poly(ethylene terephthalate) (PET) were used as templates. Information about PET membranes formation and peculiarities of their parameters control are demonstrated in Refs. [37–40]. Electrochemical deposition was carried out at voltage of 1.75 V in a two-electrode electrochemical cell using water solution of $NiSO_4 \times 6H_2O$ (100 g/l), H_3BO_3 (45 g/l) at room temperature. Process was controlled by chronoamperometric method at Agilent 34410 system.

For electrodeposition a thin gold cathode was sputtered on the rear surface of the template and it formed inside the pores a ring electrode, which predetermined the shape of synthesized NSs [41]. The deposition of metal into the pores of the PET membranes was carried out from electrolyte without its interaction with rear surface of cathode. To

ensure the absence of closing the pores with metal of the hollow channel of NTs, a sufficiently high potential was applied. It provided accelerated diffusion of metal ions into the pores, but due to the dissociation of water molecules, gas emission took part in the central of the pore. These parallel processes contributed to the reduction of metal near the pore walls with the formation of a tubular form of NSs. The deposition process and the influence of the synthesis parameters on the morphological features of nickel NTs were considered in detail in Ref. [42].

NTs were extracted from PET templates by etching of polymer in a solution of 5 M NaOH at 50 °C for an hour in ultrasonic bath. Residues of the alkaline solution were neutralized in 1% solution of acetic acid and deionized water. The washing procedure was carried out three times to completely purify NTs from the residues of alkali and acid.

1.3. Degradation mechanism study

To study the degradation process in various media, Ni NTs extracted from polymer templates at mass concentration of 0.0005 g per 10 ml of water solution were used. Three aqueous solutions with pH from 1 (strong acid medium) to 7 (neutral medium) were employed. The hydrogen ion concentration in the solutions was gradually increased using weakly concentrated (0.01 M) hydrochloric acid, which was added in small doses (droplets) to the continuously stirred aqueous solution. The values of pH were controlled using pH meter (Hanna Instruments HI2210-02). After attaining the desired pH, pH value was additionally checked using a universal indicator paper. Extracted from PET template Ni NTs were placed in the aqueous solutions with pH for the time up to 20 days. The NTs structure and morphology were investigated after each time interval.

1.4. Surface coating

To demonstrate possible ways of Ni NTs surface protection from the influence of the external environment, the surface of NTs was coated with gold, (3-aminopropyl)trimethoxysilane (APTMS) and poly(methyl methacrylate) (PMMA). The Au coating was formed in two different methods. The first is in the coating of NTs with gold due to the reduction of the Au ions on the metal surface, and the second – electrodeposition of Ni NTs inside gold NTs, produced by wet-chemistry method.

For the obtaining of the gold coating on the Ni NTs surface the electroless wet-chemical method was used. Deposition was carried out from the aqueous solution of the gold chloride 0.02 M and hydrofluoric acid 5 M. The process temperature was 35 °C during 1 min.

Growth of Ni NTs inside the Au NTs consisted of the following stages: (1) sensitization, (2) activation, (3) synthesis of Au NTs and (4) electrodeposition of Ni NTs inside gold one. For sensitization, the PET membrane was placed in a hydrochloric acid solution of bivalent tin, where it was held for 15 min at room temperature to form Sn nuclei on the pores surface. The activation of the template surface was carried out in a solution: 0.6 M $AgNO_3$ - 1 ml, 20% NH_4OH + 0.12 M $MgSO_4{\cdot}7H_2O$ – 1 ml, 2.08 M $KNaC_4O_6H_4$ – 1 ml and deionized water – 14 ml for 3 min at room temperature. The deposition of gold NTs was carried out chemically in a gold-plating solution of 1 ml of $Na_3[Au(SO_3)_2]$ with 10 ml of solution (0.127 M Na_2SO_3, 0.625 M formaldehyde and 0.025 M $NaHCO_3$) at pH = (11–12). Precipitation was carried out for 24 h at a temperature of 4–6 °C. Synthesis of NTs inside the gold was carried out according to the electrodeposition route described before.

The amine functionalization of NTs surface was carried out by adding 1 ml of Ni NTs APTMS with concentration of 20 mM in ethanol. The reaction mixture was placed in an ultrasound bath for 1–2 min and then kept NTs in these solutions for 12 h at room temperature. After the Ni NTs amination procedure samples were washed in ethanol and dried in air.

Covering of Ni NTs with polymer was carried out using PMMA. The coating was realized by placing NTs in a 10% solution of PMMA in dichloroethane for 24 h, then the polymer coated NTs were washed in dichloroethane, ethanol and dried.

1.5. Characterization

Characterization of structural features was conducted by scanning electron microscopy method (SEM, Hitachi TM3030), energy dispersive X-Ray analysis (EDX, Bruker XFlash MIN SVE), X-ray diffraction analysis (XRD, Bruker D8 ADVANCE) using Cu K_α radiation. For spectra analysis, Bruker AXSDIFFRAC.EV Av.4.2 and an international database ICDD PDF-2 were used. Control of internal diameters and estimation of wall thicknesses was conducted by methods of gas permeability (Sartocheck® 3 Plus 16290). For control of resulted polymer coating Fourier-transform infrared (FTIR) spectra were recorded on Agilent Technologies Cary 600 Series FTIR Spectrometer with Single Reflection Diamond ATR accessory (Gladiatr, PIKE). Measurements were taken in the wavelength range from 400 cm^{-1} to 3000 cm^{-1}. All spectra (32 scans at 4.0 cm^{-1} resolution and rationed to the appropriate background spectra) were recorded at room temperature. Data processing was carried out by Agilent Resolution Pro software.

2. Results

2.1. Nanotubes formation

Typical SEM images of nickel NSs obtained by the template synthesis are shown in Fig. 1 (the PET template is chemically removed).

The synthesized NSs had the form of hollow tubes (insert to Fig. 2) with a length corresponding to the original thickness of the PET template (11.8 ± 0.2 μm) and external diameters corresponding to pore diameters of 380 ± 20 nm. Considering the insufficient resolution of SEM images, the determination of the internal diameters of NTs in the pores of the PET template was carried out by the manometric method of determining gas permeability [37]. The internal diameters of nickel NTs were 160 ± 20 nm, corresponding wall thickness is approximately equal to 110 nm. The determination of the elemental composition by the EDX method has shown that NTs consist of pure nickel, and they are free from any impurities.

2.2. Degradation mechanism study

The dynamics of the surface change of nickel NTs after their exposition in solutions with pH = 1...7 for up to 20 days was controlled

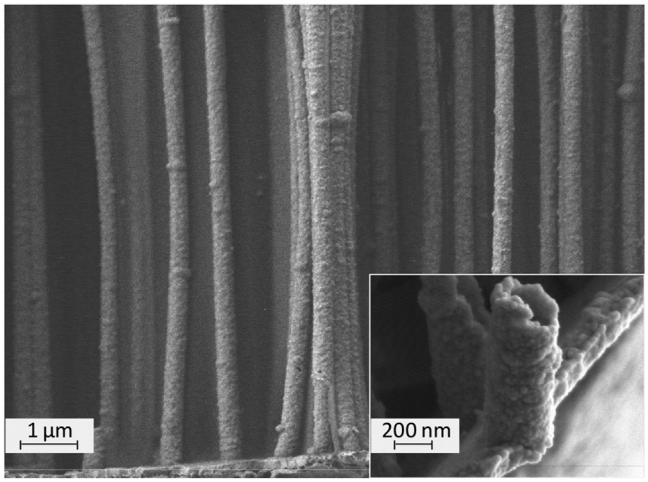

Fig. 2. Typical SEM image of array of nickel nanotubes after removal from polymer template and an enlarged part of a broken nanotube (insert to the figure).

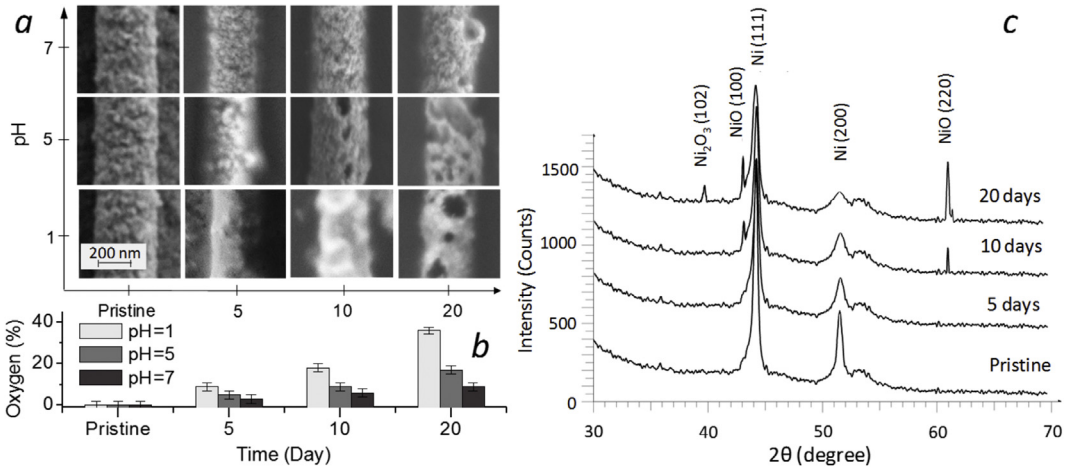

Fig. 3. Degradation of Ni nanotubes depending on the time of exposition in solutions: (a) SEM images of the evolution of nickel nanotubes morphology exposition in media with different pH (scale is same for all SEM images); (b) Dependence of the oxygen in the nanotubes composition exposition in media with different pH, calculated from EDX results, (c) XRD spectra of nickel nanotubes in solution with pH = 1.

by SEM and EDX methods (Fig. 3a).

It is evident that changes in the morphology of NTs occur in all solutions during long-term exposition, while the largest surface transformation is observed in acidic media (pH = 1). Already on the fifth day, according to EDX, the oxygen content in NTs is about 10% (Fig. 3b). On the tenth day, the oxygen content increases to 18%. Partial destruction of the walls is observed after 20 days, and the structure of NTs contains 36% of atomic oxygen. In solutions with pH = 5 and pH = 7, morphology changes more slowly: on the fifth day, oxygen content on the surface of NTs does not exceed 5% and 3%, on the 10th day 9% and 6%, and on the 20th day - 17% and 9%, respectively.

X-ray diffraction spectra (Fig. 3c and Supplementary 1), allowed to determine the dynamics of the changes in the structure of nickel NTs. The large ratio of peaks (111) and (200) in pristine NTs indicates that they have the preferred growth direction (111). The XRD spectrum contains broadened peaks; it is typical for diffraction on nanoscale objects. NTs have a face-centered cubic (FCC) lattice structure with the parameter $a = 3.5192 \pm 0.0007$ Å.

The result of exposition in a neutral solution (pH = 7) is a slight increasing of the parameter a from 3.5192 to 3.5237 Å (Table 1). Low intensity of NiO peaks with orientation (220) appear on the twentieth day. In solution with pH = 5, an increasing of the parameter a from 3.5192 to 3.5322 Å is observed. The appearance of nickel oxide (II) peaks occurs on the tenth day, their intensity increases with elongation of exposition time.

Changes in nickel NTs in solution with pH = 1 have the same character as in less acidic media, but they are more pronounced. Exposition in an acidic solution leads to increasing of the lattice parameter a (from 3.5192 to 3.5511 Å). After 5 days under influence of media, the intensity of the main peaks (111) and (200) decreases with their simultaneous broadening, while the appearance of new peaks on the XRD spectrum is not observed. Increasing of the exposition time to 10 days leads not only to decreasing of the intensity of the main peaks (111) and (200), but also to the appearance of peaks at $2\theta = 43.3^\circ$ and 62.8° corresponding to the formation of a new phase, nickel oxide (II). For 20 days exposition samples, the intensity of the NiO peaks increases; it corresponds to the results of EDX and indicates an increasing of oxide phase amount. The appearance of nickel oxide (III) phase ($2\theta = 39.3^\circ$) is also recorded on the XRD spectra.

Table 1
Changes in the crystallite size and degree of crystallinity.

Day	a, Å			Crystallinity, %		
	pH = 1	pH = 5	pH = 7	pH = 1	pH = 5	pH = 7
Pristine	3.5192	3.5192	3.5192	89	89	89
5	3.5211	3.521	3.5201	75	85	87
10	3.5371	3.5242	3.5211	73	82	85
20	3.5511	3.5322	3.5237	67	78	83

An analysis of the shape and width of the peaks on XRD patterns with the use of symmetric pseudo-Voigt functions made it possible to estimate the degree of crystallinity and also to trace the dynamics of crystal structure amorphization in media with different pH. The change in the lattice parameter a and in the crystallinity degree are presented in Table 1.

For media with pH = 5, the crystallinity degree decreases to 82% for 10 days and 78% for 20 days. For media with pH = 1 the crystallinity diminishes from 89% for the original sample to 73% for 10 days and 67% on day 20.

From the point of view of chemical reactions, the interaction of Ni NTs with media characterized by different acidities (pH was regulated by the addition of hydrochloric acid) can be described by the following reactions:

$$Ni + H_2O \leftrightarrow Ni^{2+} + 2e^- + H_2O \leftrightarrow NiO + H_2 \quad (1)$$

$$2Ni + 3H_2O \leftrightarrow 2Ni^{2+} + 3H_2O \leftrightarrow Ni_2O_3 + 3H_2 \quad (2)$$

$$2Ni + O_2 \leftrightarrow 2NiO \quad (3)$$

$$4Ni + 3O_2 \leftrightarrow 2Ni_2O_3 \quad (4)$$

$$NiO + 2HCl \leftrightarrow NiCl_2 + H_2O \quad (5)$$

$$Ni_2O_3 + 6HCl \leftrightarrow 2NiCl_3 + 3H_2O \quad (6)$$

$$NiO + H_2O \leftrightarrow Ni(OH)_2 \quad (7)$$

$$2NiO + H_2O \leftrightarrow Ni_2O_3 + H_2 \quad (8)$$

According to the Pourbaix diagram for the Ni–H_2O system [43], during the interaction of nickel with solutions (pH < 3), active dissolution of nickel occurs with forming of Ni^{2+} ions. That's why stable nickel oxides, which are registered on the XRD-patterns (Fig. 3c), can not be formed thermodynamically. Using Pourbaix diagram to analyze the processes occurring during the interaction of Ni NTs with media, it is necessary to bear in mind that the potential-pH diagrams do not take into account kinetics of the reactions and the presence of other ions (for example, chloride ions) in solutions. Thus, this interaction between Ni NTs and media with high content of Cl^- ions initiates reactions 5 and 6. A great content of chloride ions promotes more active formation of nickel oxides [44], that is observed in our case as well.

At pH values of 1...7 on the Pourbaix diagrams presents «the passivation region». In acidic media the primary passivating film is formed by nickel oxides (reactions 2, 3, 4 and 8). This film protects the sample from the electrolyte influence. In ideal systems, where only the thermodynamics of the process is taken into account, the protective layers are stable. In real systems, where kinetics plays an important role, during the corrosion of NTs walls the probability of oxides formation in the sample volume is high. In work [45], devoted to researching of potential-acidity diagram in real conditions, it was shown that at low pH, zones of pitting corrosion are formed. Destruction of the passivation film promotes the penetration of oxygen into the sample volume. However, the rate of volumetric oxidation is usually low, it is observed in a series of experiments with nickel NTs at various pH.

It should be noted that for low pH values, Ni_2O_3 (reactions 2, 4, 8) can be stable, that promotes pitting corrosion. However, it is important to clarify that in our case the Ni_2O_3 phase is formed only in solutions (pH = 1) with an exposition time of not less than 20 days (Fig. 3c and Supplementary 1). Most likely, it occurs due to the fact that during prolonged contact with an acidic media, the NTs undergo greater destruction than in media (pH > 1) and with an exposition time of less than 20 days. Accordingly, all the main occurring processes are appeared in greater degree, and the probability of Ni_2O_3 formation in such conditions is higher than in more acidic solutions and in the case of lower exposition time.

At pH = 7, the primary passivating film is hydroxide $Ni(OH)_2$ (7), which can be formed in the presence of Ni^{2+} ions on the metal surface. This hydroxide provides relatively reliable protection against general corrosion. The formation of oxides in case of the long exposition times at pH = 7 can be explained by the fact that the necessary distances for macro- and microdiffusion are small due to the small wall thickness and also due to the features of NTs such as a high ratio of surface area to volume, the presence of residual stresses and other defects, which influence on the mechanisms of ongoing processes. The penetration of oxygen into the walls occurs from the side of the NTs surface in the direction perpendicular to its main axis, as evidenced by the appearance on the XRD-patterns (Supplementary 1) of the NiO peak (220) in the absence (100), when the NTs were exposition for 20 days in a solution with pH = 7.

Reducing the degree of crystallinity (Table 1) below 73% leads to a high degree of amorphization of the structure due to the formation of oxide compounds NiO and Ni_2O_3. During the comparing these data with SEM images (Fig. 3a), it can be concluded that the formation of oxide phases, their transition into water-soluble salts $NiCl_2$ (5) and $NiCl_3$ (6) in acidic solutions and these salts subsequent washing out leads to the destruction of the nickel NTs walls. It should be noted that when NTs are exposition in acidic solutions for less than 10 days, essential changes in surface are not detected, although the degree of crystallinity is 75%. Taking into account the EDX data (Fig. 3b), which indicate the presence of oxygen in the structure of NTs, it can be assumed that point defects and nanosized inclusions of the oxide phase are formed, and they are amorphous and are not expressed as isolated peaks in the XRD spectra (Fig. 3c and Supplementary 1).

The exposition of NTs in solutions with different acidities leads to increasing of the crystal lattice parameter (Table 1). Changes in the parameter a can indicate an increasing of both the number of defects and appearance of stresses with a rising of the content of oxide compounds in nickel crystallites. As a result, NTs wall are formed as polycrystalline.

The deficiency of structure is estimated based on the concentration of vacancies, which is determined using formula [46]:

$$C_v = 3\left(\frac{\Delta L}{L} - \frac{\Delta a}{a}\right), \quad (9)$$

if $\frac{\Delta L}{L}$ – is changing of the average size of crystallites, $\frac{\Delta a}{a}$ – is changing of the average of crystal lattice parameter.

The calculation of the average stress in the crystal structure is carried out using formula [28]:

$$S = \varepsilon.\frac{Y}{2G}, \quad (10)$$

if $\varepsilon = |\frac{a_0 - a}{a_0}|$ – is coefficient of structure deformation, a_0 and a – the reference and experimentally obtained values of the lattice parameter, Y – elastic modulus, G – Poisson's ratio for explored metal.

Table 2
Dynamics of changes of defects concentration and in the crystal structure.

Day	Defects concentration			Average stress		
	pH = 1	pH = 5	pH = 7	pH = 1	pH = 5	pH = 7
Pristine	–	–	–	–	–	–
5	0.504	0.243	0.133	0.390	0.370	0.018
10	1.344	0.760	0.491	3.710	1.030	0.390
20	2.002	1.355	0.910	6.530	2.670	0.920

Dynamics of changes in the concentration of vacancies and the average stress in the crystal structure during the exposition of nickel NTs in different acidity media are shown in Table 2.

It can be seen a sharp increasing of the concentration of vacancies in the crystal structure is observed in all solutions, and already at 5 days of exposition $C_V = 0.504$ in a solution with pH = 1. It can be explained by the realization of the Kirchendall effect [47,48]. These processes are accompanied by the formation of voids and can contribute to the destruction of NTs walls. The formation of defects leads to extension of deformation of the crystal lattice, which is reflected as changes in the shape of the peaks on XRD patterns (Fig. 3c and Supplementary 1) and their deviations from the symmetrical shape.

Summarizing the obtained data, it can be assumed that the oxidation of nickel NTs will occur according to the scheme shown in Fig. 4. The formation of water-insoluble nickel oxides and hydroxides in neutral solutions leads to passivation of the NTs surface, which significantly reduces their reactivity. The small thickness of the NTs walls, as well as the general imperfection of nanoscale structures possessing a large share of surfaces, residual stresses and other defects, leads to the formation of the oxide phase at large exposition times due to macro- and microdiffusion of oxygen into the walls.

The interaction of nickel NTs with solutions (pH = 5) leads to passivation of the surface with formation of nickel (II) oxide, as well as formation of point defects and nanosized oxide inclusions in the NTs structure (pitting effect). Such kinds of defects grow in size with the increasing of the interaction time and spread deep into the NTs walls. The presence of chloride ions contributes to the more active formation of nickel oxides, as well as the formation of a water-soluble salt of $NiCl_2$, and following washing out of them leads to the through corrosion of the nickel NTs walls.

In strongly acidic media (pH = 1), the structure of nickel NTs changes in the same mechanism as it shown below. However, a large concentration of chloride ions promotes an increasing of the degradation rate of NTs walls with the formation of nickel (III) oxides during prolonged exposition. In the presence of Ni_2O_3, in addition to $NiCl_2$, water-soluble salt of $NiCl_3$ is forming too; it causes a faster destruction of the walls. It should be noted that the presence of a hollow channel inside NTs leads to uneven destruction along their length.

2.3. Surface coating

Taking into account NTs degradation, for their using it is necessary to cover them with various functional coatings. It is interesting that coatings can provide new bonds to attach functional groups to their surfaces (anticancer drugs or antibodies), that is extremely important for NTs bioapplications [49]. To show possible ways of NTs coatings we considered three main types of metallic nanomaterials functionalization: gold, organosilicon compounds and polymers coatings. Schematic

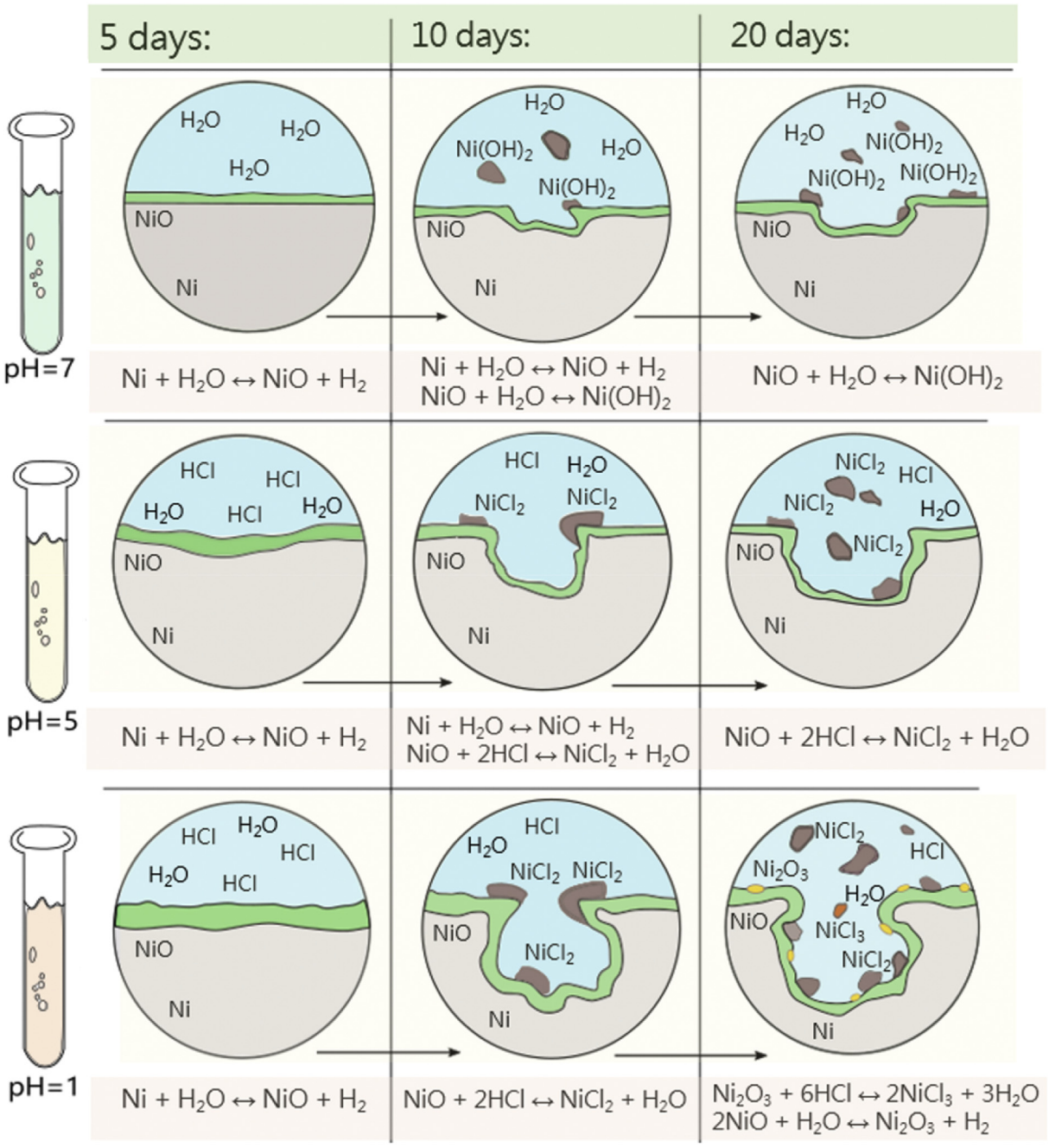

Fig. 4. Schematic representation of degradation processes on the surface of Ni NTs in media with pH = 1, 5 and 7 (exposition time of 5, 10 and 20 days).

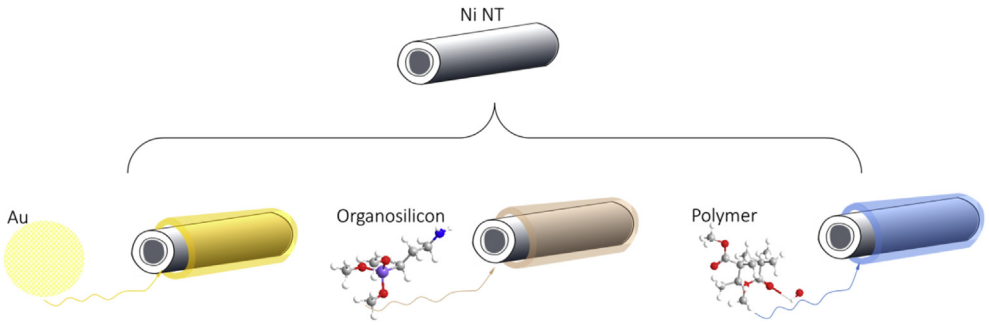

Fig. 5. Schematic representation of Ni NTs surface protection with gold, organosilicon compounds and polymers coatings. (For interpretation of the references to colour in this figure legend, the reader is referred to the Web version of this article.)

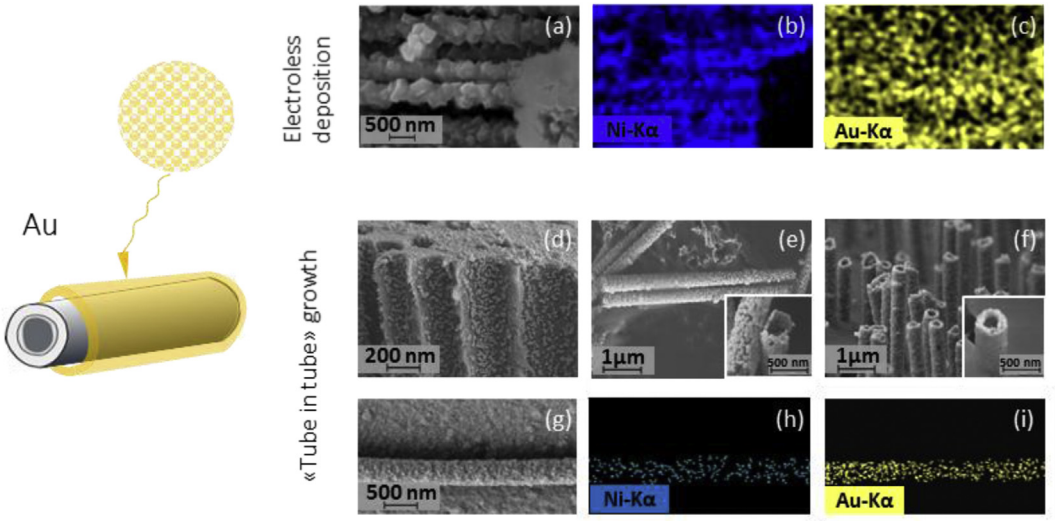

Fig. 6. Au/Ni NTs obtained by the electroless wet-chemical method: (a) SEM image and (b, c) EDX mapping in the regime of Ni and Au detection. Main stages of "tube on tube" Au/Ni NTs formation: (d) cross-section of activated PET template with Ag nanoparticles, (e) gold NTs extracted from the PET template, (f) Ni NTs grown up in Au one. (g) SEM image of Au/Ni NT with (h, i) EDX mapping in the regime of Ni and Au detection. (For interpretation of the references to colour in this figure legend, the reader is referred to the Web version of this article.)

representation of possible ways of Ni NTs surface protection with gold, organosilicone compounds and polymer coatings are presented on Fig. 5.

In present work covering with gold was produced by two methods: standard chemical technique (wet chemical reduction of metal on metal) and by using of original technique for creating multi-wall nanosystems "Ni NTs inside gold" via direct growth of 1D NTs inside the gold one. Organosilicon coating was created by polycondensation of APTMS. To functionalize the surfaces of Ni NTs with polymers was used direct reaction between the hydroxide groups formed on the surface of the NTs due to corrosion in weakly alkaline solutions and the C—O bonds that are present in the polymers, by the formation of hydrogen bonds of PMMA.

Gold coating. Electroless wet-chemical deposition implies reduction of metal on metal by reaction of replacement and provide an opportunity to obtain gold layer on the Ni NTs surface. Analysis of SEM images of Au/Ni NTs showed that gold coating of NTs surface is a continuous film consisting of individual crystallites with characteristic dimensions of 50–100 nm (Fig. 6a). EDX mapping simultaneously register nickel (Fig. 6b) and gold (Fig. 6c) that indicates the formation of a gold layer on the surface of nickel. Thus, this data shows the potential of the electroless wet-chemical method application for Ni NSs coating. However, a rather large size of the crystallites indicates that the film is a sufficiently thick and, correspondingly, it is necessary to improve deposition regimes.

Formation of Au film on the NSs surface by the "tube in tube" route implies growth of Ni NTs inside the Au NTs and consists of the fourth stages: (1) sensitization, (2) activation, (3) synthesis of Au NTs and (4) electrodeposition of Ni NTs inside gold one. The first stage is tin sensitization of PET templates, when on the pores surface forms Sn nuclei. These nuclei were used in the activation phase, as the centers of silver nanoparticles (NPs) crystallization from a solution of silver nitrate. It can be seen from (Fig. 6d) that the average size of Ag NPs formed on pores surface varies in the range of 25–30 nm. Precipitation of Au NTs in a gold-plating solution is activated due to the replacement of silver atoms by gold atoms. The SEM image (Fig. 6e) shows, that Au NTs have a granular wall structure with an individual crystallite size of about 50 nm and repeat the geometry of the template pores. The external diameter of Au NTs is about 430 nm. The internal diameter of Au NTs established by the gas permeability method, is 370 nm, it corresponds to a wall thickness about 30 nm. The formation of Au/Ni NTs with a "tube on tube" structure was performed by an electrochemical method using the same regimes as for the formation of Ni NTs in the pores of PET templates. Before electrochemical deposition a gold layer formed during chemical deposition was removed from one side of the template by etching with an ion beam. SEM images of Au/Ni NTs shown in Fig. 6f and g indicate the possibility to create « tube in tube » nanosystem. EDX mapping (Fig. 6h and i) confirms the formation of the Au film on the Ni NTs surface.

Organosilicon compound coating (APTMS). Functionalization of the surface of Ni NTs with organosilicon compound was carried out by amination reaction using APTMS. The process is based on the chemical inertness of Si—C linkages and the high reactivity of Si—O bond which readily undergoes hydrolysis and reacted with OH-terminated NTs surface. The scheme of process is shown in Fig. 7a. To confirm that samples modified with organosilicon compound were examined by SEM with EDX mapping of the surface. In the SEM image (Fig. 7b), a change of the NTs surface with respect to the uncoated sample (Fig. 2) is shown on considerably difference. EDX mapping (Fig. 7c and d) clearly shows that the organosilicon compound is localized exceptionally in the surface of the NTs.

Polymer coating (PMMA). Coating of Ni NTs with polymer was carried out by immersion in the PMMA solution. The interaction of PMMA with metallic surface takes place due to both adhesion forces and formation of hydrogen bonds of the oxidized surface of NTs with the carbonyl component of PMMA, as shown in Fig. 8a. Pretest analysis of PMMA/Ni NTs was carried out by SEM. A comparison of SEM images of coated (Fig. 8b) and non-coated NTs (Fig. 8c) demonstrates a difference in the morphology of the structure surfaces before and after functionalization. The pristine NTs have a relatively smooth surface and after PMMA coatings have uneven surface with presence of conglomerates formed as a result of the polymerization of monomers not interacted with the Ni NTs surface. FTIR-IR spectrometry confirms the formation of PMMA bonds with the NTs surface (Fig. 8d). The FTIR-IR spectrum of Ni NTs is a poorly informative curved line before coating with polymer. After functionalization the IR spectrum of Ni NTs almost completely reproduces the PMMA spectrum that indicates the successful coating of NTs with a PMMA layer. In the spectrum there are main adsorption peaks: 1150, 1180, 1220 cm^{-1} possibly related to the C—O—C stretching vibration, 1330, 750 cm^{-1} possibly attributed to the α-methyl group vibrations. The peaks at 990 cm^{-1} together with the bands at 1069 cm^{-1} and 840 cm^{-1} are the characteristic absorption vibration

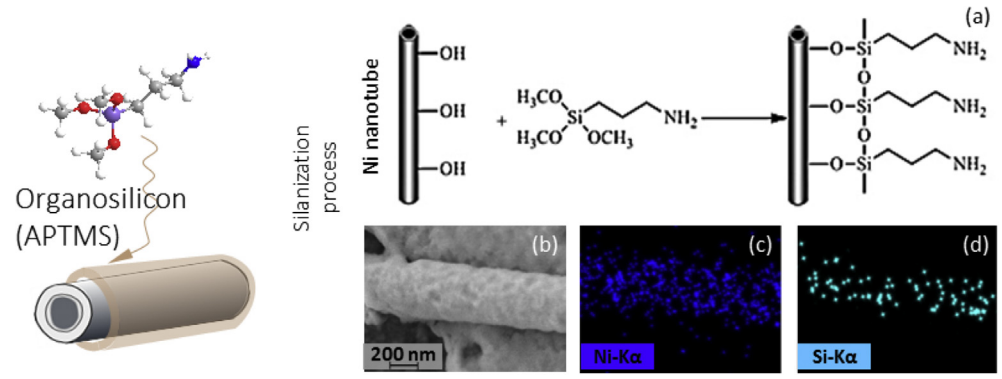

Fig. 7. (a) Scheme of Ni NTs with APTMS coating. (b) SEM image of Ni NTs with APTMS coating and (c, d) EDX mapping in the regime of Ni and Si detection.

of PMMA, 1444, 2997, 2952 cm^{-1} C–H bond, 1724 cm^{-1} related to C=O bond [50]. In this case, there is a slight shift of C=O absorption peak from 1730 cm^{-1} (for pure PMMA) to 1724 cm^{-1} (for Ni NTs-PMMA) being the evidence hydrogen bonds formation between PMMA and the surface of NTs.

Concluding the coatings described above we could add that the NTs surface coating can be considered not only from the point of view of NSs protection from the external media influence, but also for the purpose of their functionalization. Depending on the choice of material, the coatings can impart new properties to NSs or can be used for binding of cargoes. To impart new uncharacteristic properties to NSs, inorganic materials are commonly used. Such materials can significantly change electronic, photonic, magnetic, mechanical and chemical properties of the surface, for example by inhibiting agglomeration or by imparting antiseptic properties [51]. In addition, systems "NSs + inorganic coatings" are promising for application in the field of catalysis, detection (for example, using SERS), creating of nano- and microelectronics elements [52].

The surface functionalization for attachment of cargoes allows to add various types of pharmaceutical agents such as proteins, nucleic acids and drugs, which makes it possible to use the "NSs + coatings + cargo" system for targeted delivery of drugs and genes [53,54]. Organosilicon compounds and biocompatible polymer coatings are commonly used for such purposes. Modification of NTs with selected in the work organosilicon compounds (APTMS), lead to the surface coating with amine-terminated groups which have a high reactivity. It can be used to bind the protein thereto NSs [24]. When PMMA is used, amide and carboxyl groups, which allow to attach proteins and drugs, are formed. This modification of the surface makes it possible to consider "NSs + coatings + cargo" in the context of such applications as biocatalysis [55], bio-detection [56] [57] [58], biose-paration [2], delivery of drugs and genes [59], etc.

It should be noted that the data above, shows the first results of the Ni NTs surface coating with noble metal (gold), organosilicon compound (APTMS) and polymer (PMMA) and is provided to demonstrate the possibility of protecting the surface of Ni NSs from the environment effect. Detail consideration of coatings, as well as the assessment of their effectiveness in terms of protecting the surface in media with varying acidity will be given in next works.

3. Conclusion

Ni NTs with a diameter of 400 nm and a wall thickness of about 120 nm were obtained by template synthesis method. SEM, EDX, and

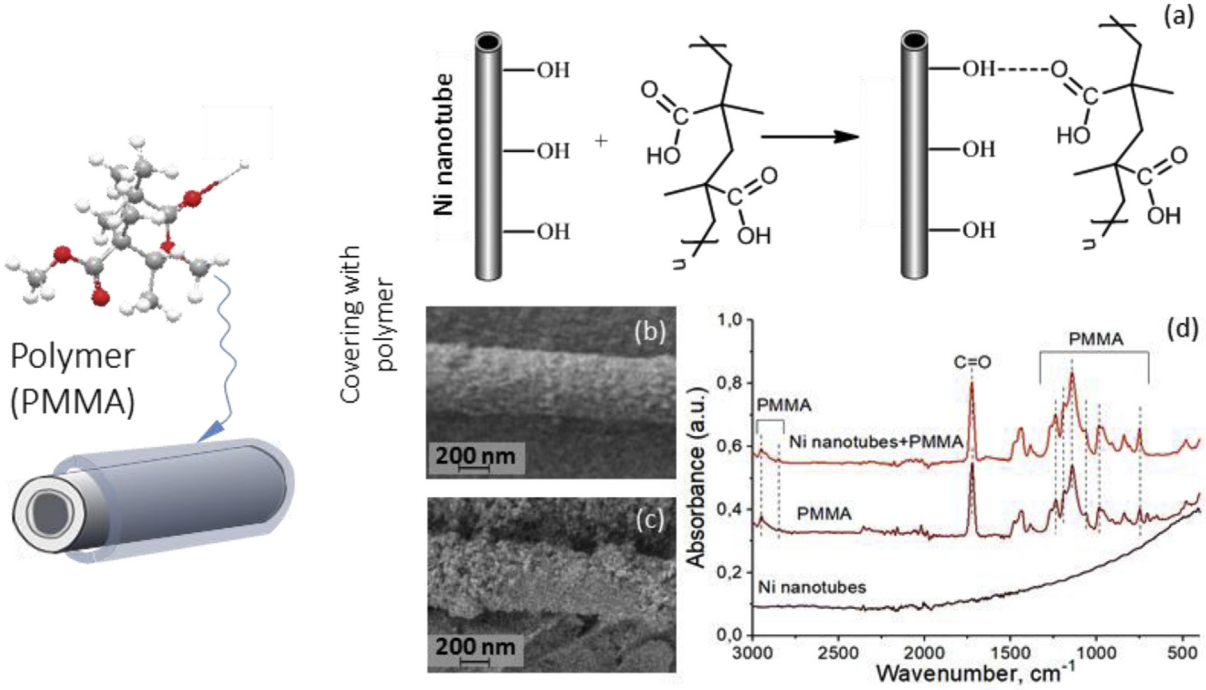

Fig. 8. (a) Scheme of Ni NTs coating with PMMA. SEM image of (b) Ni NTs and (c) PMMA/Ni system. (d) FTIR spectra of coating.

XRD investigations of the dynamics of changes in the morphology, composition, and basic structural parameters of Ni NTs when they were exposed in media with pH = 1, 5, 7 (the acidity of aqueous solutions was regulated by the addition of hydrochloric acid) up to 20 days showed that changes of NTs morphology and structure occurred in all solutions. The nature of the changes is related to the increasing of the oxygen content, which enters the crystal lattice with the formation of phases of nickel (II) and (III) oxide. The penetration of oxygen into the walls mainly occurs from the side of the NTs surface and the greatest surface degradation is observed in acid media, with an increasing of the oxygen content in the NTs structure up to 36%. According to the obtained results, the scheme of NTs degradation is proposed: passivation of the surface → formation of point defects and nanoscale inclusions → pitting → destruction. The reaction rate increases inversely proportional to the media acidity and directly proportional to the chloride ions content in the solution.

The possible ways of nickel NSs surface protection from the environment effect using coatings based on noble metal (gold), organosilicon compound (APTMS) and polymer (PMMA) were shown. For the formation of gold coating two methods were used – the standard one, consisting of using the electroless wet-chemical method, and the original one – by the "tube in tube" route. The surface protection with organosilicon compound was carried out by using APTMS which reacted with OH-terminated surface of Ni NTs. Coating with polymer was carried out by using PMMA which reacts with metallic surface due to formation of hydrogen bonds of the oxidized surface of NSs with the carbonyl component of PMMA.

Coating the Ni NSs surface allows not only to protect them from the influence of the environment, but also to form additional functional bonds. Functionalization of the surface is important from the point of view of the possibility of various substances binding to the NSs surface and can be practically used, for instance, for the targeted drug delivery, separation of biological objects, catalysis and biodetection.

Acknowledgement

The authors acknowledge the support of the work in frames of H2020 - MSCA - RISE2017 - 778308 - SPINMULTIFILM Project.

Appendix A. Supplementary data

Supplementary data related to this article can be found at https://doi.org/10.1016/j.matchemphys.2018.09.010.

References

[1] C.F. Guo, Z. Ren, Flexible transparent conductors based on metal nanowire networks, Mater. Today 18 (2014) 143–154, https://doi.org/10.1016/j.mattod.2014.08.018.
[2] D.T. Mitchell, S.B. Lee, L. Trofin, N. Li, T.K. Nevanen, H. Söderlund, C.R. Martin, Smart nanotubes for bioseparations and biocatalysis, J. Am. Chem. Soc. 124 (2002) 11864–11865, https://doi.org/10.1021/ja027247b.
[3] V. Haehnel, S. Fähler, P. Schaaf, M. Miglierini, C. Mickel, L. Schultz, H. Schlörb, Towards smooth and pure iron nanowires grown by electrodeposition in self-organized alumina membranes, Acta Mater. 58 (2010) 2330–2337, https://doi.org/10.1016/j.actamat.2009.12.019.
[4] A.K. Salem, P.C. Searson, K.W. Leong, Multifunctional nanorods for gene delivery, Nat. Mater. 2 (2003) 668–671, https://doi.org/10.1038/nmat974.
[5] H. Hillebrenner, F. Buyukserin, J.D. Stewart, C.R. Martin, Template synthesized nanotubes for biomedical delivery applications, Nanomedicine 1 (2006) 39–50, https://doi.org/10.2217/17435889.1.1.39.
[6] A. Shumskaya, E. Kaniukov, M. Kutuzau, A. Kozlovskiy, M. Zdorovets, Electrodeposited Ferromagnetic Nanotubes: Structure and Magnetic Properties, Nanomater. Appl. Prop. (NAP) (2017), https://doi.org/10.1109/NAP.2017.8190412 IEEE 7th Int. Conf. (2017) 02MFPM08-1-02MFPM08-4.
[7] S. Barth, S. Estrade, F. Hernandez-Ramirez, F. Peiro, J. Arbiol, A. Romano-Rodriguez, J.R. Morante, S. Mathur, Studies on surface facets and chemical composition of vapor grown one-dimensional magnetite nanostructures, Cryst. Growth Des. 9 (2009) 1077–1081, https://doi.org/10.1021/cg8009095.
[8] J.R. Morber, Y. Ding, M.S. Haluska, Y. Li, J.P. Liu, Z.L. Wang, R.L. Snyder, PLD-assisted VLS growth of aligned ferrite nanorods, nanowires, and nanobelts-synthesis, and properties, J. Phys. Chem. B 110 (2006) 21672–21679, https://doi.org/10.1021/jp064484i.
[9] Z. Liu, Q. Zhang, G. Shi, Y. Li, H. Wang, Solvothermal synthesis and magneto-optical properties of Zn1 − xNixO hierarchical microspheres, J. Magn. Magn Mater. 323 (2011) 1022–1026, https://doi.org/10.1016/j.jmmm.2010.12.011.
[10] Z. Hua, S. Yang, H. Huang, L. Lv, M. Lu, B. Gu, Y. Du, Metal nanotubes prepared by a sol–gel method followed by a hydrogen reduction procedure, Nanotechnology 17 (2006) 5106–5110, https://doi.org/10.1088/0957-4484/17/20/011.
[11] D. Zhou, T. Wang, M.G. Zhu, Z.H. Guo, W. Li, F.S. Li, Magnetic interaction in FeCo alloy nanotube array, Jpn. Mag. 16 (2011) 413–416, https://doi.org/10.4283/JMAG.2011.16.4.413.
[12] A. V Trukhanov, S.S. Grabchikov, S.A. Sharko, S. V Trukhanov, K.L. Trukhanova, O.S. Volkova, A. Shakin, Magnetotransport properties and calculation of the stability of GMR coefficients in CoNi/Cu multilayer quasi-one-dimensional structures, Mater. Res. Express 3 (2016) 065010, , https://doi.org/10.1088/2053-1591/3/6/065010.
[13] V.A. Ketsko, E.N. Beresnev, M.A. Kop'eva, L.V. Elesina, A.I. Baranchikov, A.I. Stognii, A.V. Trukhanov, N.T. Kuznetsov, Specifics of pyrohydrolytic and solid-phase syntheses of solid solutions in the (MgGa2O4) x (MgFe2O4)1 − x system, Russ. J. Inorg. Chem. 55 (2010) 427–429, https://doi.org/10.1134/S0036023610030216.
[14] X. Li, X. Wei, Y. Ye, Template electrodeposition to cobalt-based alloys nanotube arrays, Mater. Lett. 63 (2009) 578–580, https://doi.org/10.1016/j.matlet.2008.12.002.
[15] V.A. Online, X. Li, K. Wu, Y. Ye, X. Wei, Gas-assisted growth of boron-doped nickel nanotube arrays: rapid synthesis, growth mechanisms, tunable magnetic properties, and super-efficient reduction of 4-nitrophenol †, (2013), pp. 3648–3653, https://doi.org/10.1039/c3nr00411b.
[16] X.-Z. Li, K.-L. Wu, Y. Ye, X.-W. Wei, Controllable synthesis of Ni nanotube arrays and their structure-dependent catalytic activity toward dye degradation, CrystEngComm 16 (2014) 4406, https://doi.org/10.1039/c4ce00225c.
[17] L.G. Vivas, Y.P. Ivanov, D.G. Trabada, M.P. Proenca, O. Chubykalo-Fesenko, M. Vázquez, Magnetic properties of Co nanopillar arrays prepared from alumina templates, Nanotechnology 24 (2013) 105703, https://doi.org/10.1088/0957-4484/24/10/105703.
[18] D. Yakimchuk, E. Kaniukov, V. Bundyukova, L. Osminkina, S. Teichert, S. Demyanov, V. Sivakov, Silver nanostructures evolution in porous SiO 2 / p -Si matrices for wide wavelength surface-enhanced Raman scattering applications, MRS Commun. 8 (2018) 95–99, https://doi.org/10.1557/mrc.2018.22.
[19] E. Kaniukov, D. Yakimchuk, G. Arzumanyan, H. Terryn, K. Baert, A. Kozlovskiy, M. Zdorovets, E. Belonogov, S. Demyanov, Growth mechanisms of spatially separated copper dendrites in pores of a SiO 2 template, Philos. Mag. 97 (2017) 2268–2283, https://doi.org/10.1080/14786435.2017.1330562.
[20] J.J. Murphy, P. Melchiorre, Organic chemistry: light opens pathways for nickel catalysis, Nature 524 (2015) 297–298, https://doi.org/10.1038/nature15200.
[21] S.S. Grabchikov, A.V. Trukhanov, S.V. Trukhanov, I.S. Kazakevich, A.A. Solobay, V.T. Erofeenko, N.A. Vasilenkov, O.S. Volkova, A. Shakin, Effectiveness of the magnetostatic shielding by the cylindrical shells, J. Magn. Magn Mater. 398 (2016) 49–53, https://doi.org/10.1016/j.jmmm.2015.08.122.
[22] L. Zhang, T. Petit, K.E. Peyer, B.J. Nelson, Targeted cargo delivery using a rotating nickel nanowire, Nanomed. Nanotechnol. Biol. Med. 8 (2012) 1074–1080, https://doi.org/10.1016/j.nano.2012.03.002.
[23] T.N. Narayanan, M.M. Shaijumon, P.M. Ajayan, M.R. Anantharaman, Synthesis of high coercivity core–shell nanorods based on nickel and cobalt and their magnetic properties, Nanoscale Res. Lett. 5 (2010) 164–168, https://doi.org/10.1007/s11671-009-9459-7.
[24] A.L. Kozlovskiy, I.V. Korolkov, G. Kalkabay, M.A. Ibragimova, A.D. Ibrayeva, M.V. Zdorovets, V.S. Mikulich, D.V. Yakimchuk, A.E. Shumskaya, E.Y. Kaniukov, Comprehensive study of Ni nanotubes for bioapplications: from synthesis to payloads attaching, J. Nanomater. 2017 (2017), https://doi.org/10.1155/2017/3060972.
[25] F. Nasirpouri, M.R. Sanaeian, A.S. Samardak, E.V. Sukovatitsina, A.V. Ognev, L.A. Chebotkevich, M.G. Hosseini, M. Abdolmaleki, An investigation on the effect of surface morphology and crystalline texture on corrosion behavior, structural and magnetic properties of electrodeposited nanocrystalline nickel films, Appl. Surf. Sci. 292 (2014) 795–805, https://doi.org/10.1016/j.apsusc.2013.12.053.
[26] A. Kozlovskiy, M. Zdorovets, A. Shumskaya, E. Kanyukov, M. Kutuzau, Synthesis and Properties of Ni x / Au 1-x Nanotubes, Nanomater. Appl. Prop. (NAP) (2017), https://doi.org/10.1109/NAP.2017.8190333 IEEE 7th Int. Conf. (2017) 04NB21-1-04NB21-3.
[27] K. Kasprzak, Nickel carcinogenesis, Mutat. Res. Mol. Mech. Mutagen. 533 (2003) 67–97, https://doi.org/10.1016/j.mrfmmm.2003.08.021.
[28] T. Ahmad, H. Bae, I. Rhee, Y. Chang, S.-U. Jin, S. Hong, Gold-coated iron oxide nanoparticles as a T_2 contrast agent in magnetic resonance imaging, J. Nanosci. Nanotechnol. 12 (2012) 5132–5137, https://doi.org/10.1166/jnn.2012.6368.
[29] S. Moraes Silva, R. Tavallaie, L. Sandiford, R.D. Tilley, J.J. Gooding, Gold coated magnetic nanoparticles: from preparation to surface modification for analytical and biomedical applications, Chem. Commun. 52 (2016) 7528–7540, https://doi.org/10.1039/C6CC03225G.
[30] B. Wildt, P. Mali, P.C. Searson, Electrochemical template synthesis of multisegment nanowires: fabrication and protein functionalization, Langmuir 22 (2006) 10528–10534, https://doi.org/10.1021/la061184j.
[31] A. Shumskaya, E. Kaniukov, M. Kutuzau, V. Bundyukova, A. Kozlovskiy, D. Borgekov, I. Kenzhina, Influence of media with different acidity on structure of FeNi nanotubes, EPJ Web Conf. 177 (2018) 1003, https://doi.org/10.1051/epjconf/201817701003.

[32] Y.-J. Cheng, G.-F. Luo, J.-Y. Zhu, X.-D. Xu, X. Zeng, D.-B. Cheng, Y.-M. Li, Y. Wu, X.-Z. Zhang, R.-X. Zhuo, F. He, Enzyme-Induced and tumor-targeted drug delivery system based on multifunctional mesoporous silica nanoparticles, ACS Appl. Mater. Interfaces 7 (2015) 9078–9087, https://doi.org/10.1021/acsami.5b00752.
[33] A. El Harrak, G. Carrot, J. Oberdisse, J. Jestin, F. Boué, Atom transfer radical polymerization from silica nanoparticles using the 'grafting from' method and structural study via small-angle neutron scattering, Polymer 46 (2005) 1095–1104, https://doi.org/10.1016/j.polymer.2004.11.046.
[34] J. Safari, Z. Zarnegar, Advanced drug delivery systems: nanotechnology of health design A review, J. Saudi Chem. Soc. 18 (2014) 85–99, https://doi.org/10.1016/j.jscs.2012.12.009.
[35] P.H. Dussault, Y. Osada, Y.M. Chen, Chem Soc Rev Chemistry and Their Potential Applications, (2014), https://doi.org/10.1039/c4cs00219a.
[36] R. Messing, N. Frickel, L. Belkoura, R. Strey, H. Rahn, S. Odenbach, A.M. Schmidt, Cobalt Ferrite Nanoparticles as Multifunctional Cross-linkers in PAAm Ferrohydrogels, (2011), pp. 2990–2999.
[37] E.Y. Kaniukov, E.E. Shumskaya, D.V. Yakimchuk, A.L. Kozlovskiy, M.A. Ibragimova, M.V. Zdorovets, Evolution of the polyethylene terephthalate track membranes parameters at the etching process, J. Contemp. Phys. (Armenian Acad. Sci. 52 (2017) 155–160, https://doi.org/10.3103/S1068337217020098.
[38] A. Kozlovskiy, K. Borgekov, M. Zdorovets, E. Arkhangelsky, A. Shumskaya, E. Kaniukov, Application of ion-track membranes in processes of direct and reverse osmosis, Proc. Natl. Acad. Sci. Belarus. Phys. Ser. 1 (2017) 45–51.
[39] I.V. Korolkov, A.A. Mashentseva, O. Güven, M.V. Zdorovets, A.A. Taltenov, Enhancing hydrophilicity and water permeability of PET track-etched membranes by advanced oxidation process, Nucl. Instrum. Methods Phys. Res. Sect. B Beam Interact. Mater. Atoms 365 (2015) 651–655, https://doi.org/10.1016/j.nimb.2015.10.031.
[40] I.V. Korolkov, O. Güven, A.A. Mashentseva, A.B. Atıcı, Y.G. Gorin, M.V. Zdorovets, A.A. Taltenov, Radiation induced deposition of copper nanoparticles inside the nanochannels of poly(acrylic acid)-grafted poly(ethylene terephthalate) track-etched membranes, Radiat. Phys. Chem. 130 (2017) 480–487, https://doi.org/10.1016/j.radphyschem.2016.10.006.
[41] I.V. Korolkov, D.B. Borgekov, A.A. Mashentseva, O. Güven, A.B. Atıcı, A.L. Kozlovskiy, M.V. Zdorovets, The effect of oxidation pretreatment of polymer template on the formation and catalytic activity of Au/PET membrane composites, Chem. Pap. (2017).
[42] A.L. Kozlovskiy, D.I. Shlimas, E.E. Shumskaya, E.Y. Kaniukov, M.V. Zdorovets, K.K. Kadyrzhanov, Effect of parameters of electroplating on structural and morphologic features of nickel nanotubes, Phys. Met. Metallogr. 118 (2017) 174–179, https://doi.org/10.1134/S0031918X17020065.
[43] L.L. SHREIR, Corrosion in aqueous solutions, Corrosion, Elsevier, 1976, , https://doi.org/10.1016/B978-0-408-00109-0.50013-4 p. 1:52-1:113.
[44] A. Bouzoubaa, B. Diawara, V. Maurice, C. Minot, P. Marcus, Ab initio study of the interaction of chlorides with defect-free hydroxylated NiO surfaces, Corrosion Sci. 51 (2009) 941–948, https://doi.org/10.1016/j.corsci.2009.01.028.
[45] S.J. Lennon, F.P.A. Robinson, The experimental determination of potential-pH diagrams for the Ni-H2O and low alloy steel-H2O systems, Corrosion Sci. 26 (1986) 995–1007, https://doi.org/10.1016/0010-938X(86)90129-0.
[46] R. Andrievski, A. Khatchoyan, Nanomaterials in Extreme Environments, Springer International Publishing, Cham, 2016, https://doi.org/10.1007/978-3-319-25331-2.
[47] H.J. Fan, U. Gösele, M. Zacharias, formation of nanotubes and hollow nanoparticles based on kirkendall and diffusion processes: a review, Small 3 (2007) 1660–1671, https://doi.org/10.1002/smll.200700382.
[48] R. Nakamura, J.-G. Lee, H. Mori, H. Nakajima, Oxidation behaviour of Ni nanoparticles and formation process of hollow NiO, Philos. Mag. A 88 (2008) 257–264, https://doi.org/10.1080/14786430701819203.
[49] S.E. Krown, D.W. Northfelt, D. Osoba, J.S. Stewart, Use of liposomal anthracyclines in Kaposi's sarcoma, Semin. Oncol. 31 (2004) 36–52.
[50] G. Duan, C. Zhang, A. Li, X. Yang, L. Lu, X. Wang, Preparation and characterization of mesoporous zirconia made by using a poly (methyl methacrylate) template, Nanoscale Res. Lett. 3 (2008) 118–122, https://doi.org/10.1007/s11671-008-9123-7.
[51] M. Stefan, O. Pana, C. Leostean, C. Bele, D. Silipas, M. Senila, E. Gautron, Synthesis and characterization of Fe3O4-TiO2core-shell nanoparticles, J. Appl. Phys. 116 (2014), https://doi.org/10.1063/1.4896070.
[52] D. Martín-Becerra, J.M. García-Martín, Y. Huttel, G. Armelles, Optical and magneto-optical properties of Au:Co $_{nanoparticles}$ and Co:Au $_{nanoparticles}$ doped magneto-plasmonic systems, J. Appl. Phys. 117 (2015) 053101, , https://doi.org/10.1063/1.4906946.
[53] S.K. Singh, P.P. Kulkarni, D. Dash, Biomedical applications of nanomaterials: an overview, Bio-nanotechnology, Blackwell Publishing Ltd., Oxford, UK, 2013, pp. 1–32, , https://doi.org/10.1002/9781118451915.ch1.
[54] Y. Yang, A.M. Asiri, Z. Tang, D. Du, Y. Lin, Graphene based materials for biomedical applications, Mater. Today 16 (2013) 365–373, https://doi.org/10.1016/j.mattod.2013.09.004.
[55] M. Misson, H. Zhang, B. Jin, Nanobiocatalyst advancements and bioprocessing applications, J. R. Soc. Interface 12 (2014), https://doi.org/10.1098/rsif.2014.0891 20140891–20140891.
[56] S.H. Liao, K.L. Chen, C.M. Wang, J.J. Chieh, H.E. Horng, L.M. Wang, C.H. Wu, H.C. Yang, Using bio-functionalized magnetic nanoparticles and dynamic nuclear magnetic resonance to characterize the time-dependent spin-spin relaxation time for sensitive bio-detection, Sensors 14 (2014) 21409–21417, https://doi.org/10.3390/s141121409.
[57] T.A.P. Rocha-Santos, Sensors and biosensors based on magnetic nanoparticles, TrAC Trends Anal. Chem. (Reference Ed.) 62 (2014) 28–36, https://doi.org/10.1016/j.trac.2014.06.016.
[58] M.S. Vázquez, C. Zorrilla, R. Herrera, Síntesis y Propiedades Físicas y Estructurales de Nanopartículas Monodispersas de Magnetita (Fe 3 O 4), (2009), pp. 4–5, https://doi.org/10.1002/wnan.051.
[59] M.M. El-hammadi, Iron Oxide-based Multifunctional Nanoparticulate Systems for Biomedical Applications : a Patent Review (2008 – Present), (2015), pp. 1–19, https://doi.org/10.1517/13543776.2015.1028358.